Demand-Aware Beam Design and User Scheduling for Precoded Multibeam GEO Satellite Systems

Puneeth Jubba Honnaiah, Eva Lagunas, Nicola Maturo, Symeon Chatzinotas
Interdisciplinary Centre for Security, Reliability and Trust (SnT), University of Luxembourg, Luxembourg
email: {puneeth.jubba-honnaiah, eva.lagunas, nicola.maturo, symeon.chatzinotas}@uni.lu

***Abstract*—For many years, satellite footprints have been fixed from the design phase until the last day of the satellite operational life. Flexibility in coverage by means of reconfigurable beams is becoming increasingly popular thanks to the recent developments in active antenna systems. On the other hand, spatial frequency reuse combined with precoding has been shown to boost the spectral efficiency while lowering the cost per bit. In this context, and motivated by the unbalanced demand requests of the satellite users, we propose a shift from the traditional system-throughput maximization design towards a demand-Aware design, where a new beam shaping technique and user scheduling are combined to satisfy the users' demands. Supporting numerical results are provided that validate the effectiveness of the proposed beam planning and scheduling and quantify the benefits over conventional rigid techniques.**

***Index Terms*—Multibeam GEO Satellite, Beam Design, DVB-S2X, User Scheduling, Demand Adaptability, Precoding.**

I. Introduction

Motivated by its simple deployment, conventional multi-beam GEO satellite systems operate with a static and fixed beam footprint, typically of the form of regular circular beams one next to each other, regardless of the actual user demands on Earth [1]. This naive approach typically leads to unbalanced situations, where some beams with high number of users (or with high-demand users) easily reach congestion while other beams have spare capacity [2]. A more optimal approach would explicitly consider the actual user traffic demands and design the beam footprint accordingly. Hence, beam footprint design that considers the actual spatial demand distribution on Earth, targets an evenly distributed demand among all the beams of a system [3]. Such approach has only recently become possible thanks to the advances in active antenna systems for satellite communications [4], [5].

On the other hand, the spectrum scarcity combined with the ever-growing demand for high-throughput satellite services has motivated many research works on full frequency reuse and the application of precoding to mitigate the resulting co-channel interference [6]. However, the potential benefits of precoding are limited by the user scheduling. This is because typical precoding methods rely on the channel matrix inversion [7], which is not straightforwards in case of rank-deficient matrices. Hence, while many research works focus on optimal user scheduling that selects users with orthogonal channel vectors to be served simultaneously [8], [9], others focus on jointly addressing user scheduling and precoding [10]. However, considering demand satisfaction as an objective is a better approach to perform user scheduling which can be achieved by considering both user traffic demands and channel orthogonality of the scheduled users [11].

This work has been partially supported by the Luxembourg National Research Fund (FNR) under the project FlexSAT "Resource Optimization for Next Generation of Flexible SATellite Payloads" (C19/IS/13696663) and under Industrial Fellowship Scheme with industrial partner SES S.A., project title "Resource Allocation and IntErference MitiGation for demand based capAcity adaptabiLity in Satellite Communication System (REGAL)", grant FNR14147087.

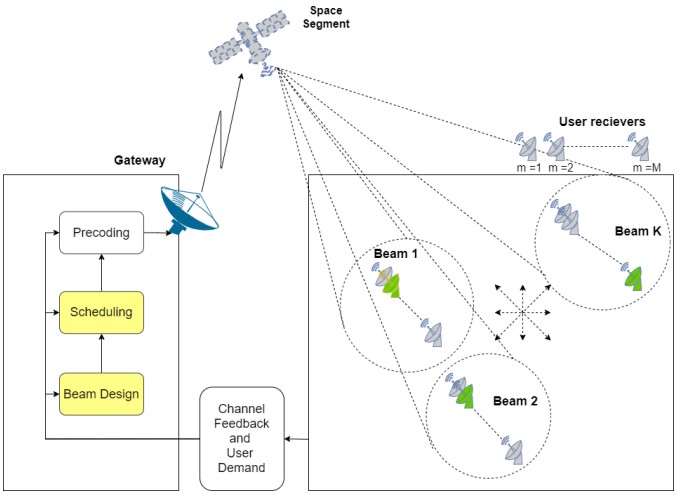

Fig. 1. GEO multibeam system architecture including beam design, user scheduling and precoding.

The contribution and novelty of this paper focuses on employing demand-driven system adaptability at multiple levels of the transmission chain and to evaluate the benefits of introducing demand considerations at these levels. Unlike previous techniques that focused on system throughput maximization [12], herein we focus on the user demand satisfaction objective. In particular, we apply demand-driven system adaptability and evaluate the demand satisfaction at beam design and user scheduling individually and jointly.

II. System Model

We consider a GEO multi-beam High Throughput Satellite (HTS) system as shown in Figure 1, employing multiple spot beams to provide the required coverage. Non-uniform spatially distributed broadband users, including mobile pedestrian users, aeronautical users and maritime users are considered. We

assume that the optimization is carried out in the ground segment. While Channel State Information (CSI) is fed back for the precoding and scheduling design, the user demand information is considered for beam and scheduling design. The space-segment consist of a programmable payload GEO satellite with Array-Fed Reflector (AFR) antennas with beam-forming capabilities.

We consider N broadband users served by K-beam Satellite system. While CSI vector is expressed as $\mathbf{h}_n \in \mathbb{C}^{K\times 1}$, $\mathbf{x} \in \mathbb{C}^{K\times 1}$ represents the precoded signal and $\mathfrak{N}_n$ represent zero-mean Additive White Gaussian Noise (AWGN). Consequently, y_n is the received signal and is expressed as,

$$y_n = \mathbf{h}_n^T \mathbf{x} + \mathfrak{N}_n, \tag{1}$$

The above model can also be expressed as,

$$\mathbf{y} = \mathbf{H}\ \mathbf{x} + \mathfrak{N}, \tag{2}$$

by considering $\mathbf{H} = \Phi\mathbf{B}$, where $\mathbf{B} = [\mathbf{b}_1 \dots \mathbf{b}_N]^T$ is the system channel matrix whose the (n, k)th component is given by,

$$[\mathbf{b}]_{n,k} = \frac{\sqrt{G_{Rn}G_{kn}}}{(4\pi\frac{\mathfrak{D}_{nk}}{\lambda})}, \tag{3}$$

where λ is the wavelength of transmission, G_{kn} are the gains defined by satellite radiation pattern, G_{Rn} is the receiver antenna gain and $\mathfrak{D}_{nk}$ is the distance between the satellite transmit antenna and user's receiving antenna. The phase matrix $\Phi \in \mathbb{R}^{K\times K}$ is expressed as,

$$[\Phi]_{xx} = e^{i\phi_x}, \forall x = 1...K \tag{4}$$

where Φ_x is a uniform random variable in $[2\pi, 0]$ and $[\phi]_{xy} = 0, \forall x \neq y$. Then, the precoded signal is given by,

$$\mathbf{x} = \mathbf{W}\ \mathbf{s}. \tag{5}$$

where $\mathbf{W}$ is the precoding matrix and $\mathbf{s}$ is the transmit symbols that satisfies $\mathbb{E}[\mathbf{s}\mathbf{s}^H] = \mathbf{I}$. The precoding matrix $\mathbf{W}$ is the MMSE precoder [13] and is expressed as,

$$\mathbf{W}_{RZF} = \eta' \boldsymbol{H}^{\boldsymbol{H}}(\boldsymbol{H}\boldsymbol{H}^{\boldsymbol{H}} + \boldsymbol{\alpha}\boldsymbol{I})^{-\mathbf{1}}, \tag{6}$$

where α is a predefined regularisation factor [14] and η is the power allocation factor defined in (7) with P_{tot} being the total available power.

$$\eta = \sqrt{\frac{P_{tot}}{\text{Trace}(\mathbf{W}\mathbf{W}^\dagger)}} \tag{7}$$

III. Problem Statement and Proposed Solution

A. Demand-Aware Beam Design

The benchmark fixed beam footprint [1] provided by European Space Agency (ESA) [6] consists of fixed number of beams (71 beams) with predetermined beam shape for a GEO 0°E satellite operating at the Ka exclusive band 19.7 to 20.2 GHz. As shown in Figure 2, we selected 6 adjacent beams out of the available 71 beams for our simulation where the blue asterisks represent the user positions. The predetermined

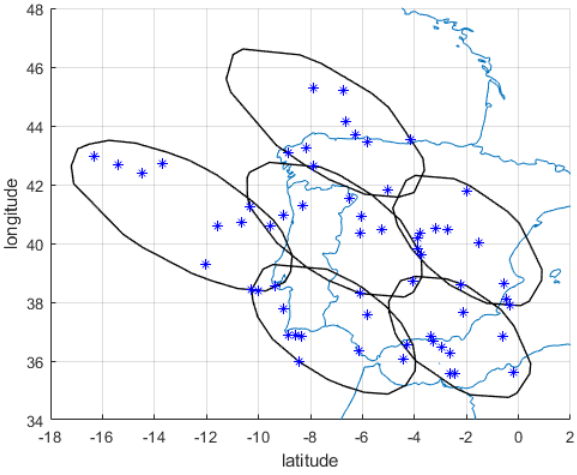

Fig. 2. Fixed Beam Footprint

beam shape or the beam footprint is fixed irrespective of the dynamic user profiles. Apparently, mobile users are not uniformly distributed and have different QoS requirements. Also, their position is a function of time. But, in the conventional beam footprint design shown in Figure 2, the offered throughput remains relatively similar across all the beams. Therefore, fixed beam plans will fail to distribute broadband traffic demand across all the beams evenly and result in either under-use the offered throughput (beam capacity is unused) or overload the beam (beam capacity is unmet).

Hence, the beam footprint has to be designed such that the occurrence of unbalanced aggregated-beam demand is avoided. To do so, we use demand-Aware adaptive beam footprint design [3]. Accordingly, we first need to find the best partition of all the users into sets of adjacent users in an euclidean distance sense such that total system demand is evenly distributed among all the sets and then, plan a beam which is suitable to serve each user set.

We define d_m as the requested traffic demand of user m, and $D_k = \sum_{m\in\mathcal{S}^k} d_m$ as the demand of beam k, where $\mathcal{S}^k$ represents the set of users belonging to beam k. Then, we define the problem using clustering approach and consider metric spaces where we endow universe $\mathcal{N}$ with a metric space $(\mathcal{X}, r)$ such that $\mathcal{N} \subseteq \mathcal{X}$, where $\mathcal{X}$ is a set of all points in a 2D Euclidean space and r is a distance metric on $\mathcal{X}$. Then to obtain the cluster sets $\{\mathcal{T}^1, \mathcal{T}^2, \dots, \mathcal{T}^K\}$ that are optimized for even demand distribution, we can define the partitioning problem using clustering as formulated in (8a).

The first constraint in (8b) ensures that all the users are under the coverage region. The second constraint in (8c) assures that any user will be served by only one beam. The third constraint mentioned in (8d) ensures that the beams have at least one user and to avoid planning beams with zero demand. In the constraint (8e), $\boldsymbol{c}_{\mathcal{T}^k}$ is two element vector in the 2D Euclidean space representing the weighted cluster centroid of the cluster k.

$$\underset{\{\mathcal{T}^1,\mathcal{T}^2...\mathcal{T}^K\}}{\text{minimize}} \quad \sum_{k=1}^{K}\sum_{m\in\mathcal{T}^k} r(\mathbf{x}_m, \boldsymbol{c}_{\mathcal{T}^k}) \left(\frac{\sum\limits_{m\in\mathcal{T}^k}(d_m)}{\sum\limits_{m=1}^{M}(d_m)}\right) \tag{8a}$$

$$\text{subject to} \quad \bigcup_{k=1}^{K}\mathcal{T}^k = \mathcal{N} \tag{8b}$$

$$\mathcal{T}^i \cap \mathcal{T}^j = \emptyset, \forall i \neq j \tag{8c}$$

$$\mathcal{T}^i \neq \emptyset, \forall i \tag{8d}$$

$$\boldsymbol{c}_{\mathcal{T}^k} = \frac{1}{\sum\limits_{m\in\mathcal{T}^k} d_m}\sum_{m\in\mathcal{T}^k} d_m\mathbf{x}_m \tag{8e}$$

To solve for (8a), we employ weighted k-means clustering using iterative Lloyd's algorithm [15] approach. Since the beam center is likely to point in the direction of the dominant group of users, centroid tessellation approach such as Lloyd's algorithm is beneficial for the beam design and the user demands can be better satisfied. The steps of Lloyd's Iteration Partition Clustering is shown in Algorithm 1. Upon termination, the Algorithm 1 provides K clusters $(\mathcal{T}^1, \mathcal{T}^2...\mathcal{T}^K)$ with cluster centroids at $\boldsymbol{c}_{\mathcal{T}^1}, \boldsymbol{c}_{\mathcal{T}^2}...\boldsymbol{c}_{\mathcal{T}^k}$ such that D_k is more evenly distributed among all the K beams.

Algorithm 1 Loyd's Iteration Partition Clustering Algorithm

[Step 1] Choose cluster centres $\{\boldsymbol{c}_{\mathcal{T}^1}, \boldsymbol{c}_{\mathcal{T}^2}...c_{\mathcal{T}^k}\}$ defined by C_s selected as per $k-means++$ Algorithm [16].

while (Cluster assignments do not change) OR (Maximum number of iterations are not reached) **do**

[Step 2] Compute distance $\mathfrak{R}_{K\times N}$ between each of $\{\boldsymbol{c}_{\mathcal{T}^1}, \boldsymbol{c}_{\mathcal{T}^2}...\boldsymbol{c}_{\mathcal{T}^k}\}$ and all of $\{\boldsymbol{x}_1, \boldsymbol{x}_2...\boldsymbol{x}_N\}$. Every element of $\mathfrak{R}_{K\times N}$ is computed using,

$$\mathfrak{R}(k,n) = ((\mathbf{x}_n - \boldsymbol{c}_{\mathcal{T}^k})(\mathbf{x}_n - \boldsymbol{c}_{\mathcal{T}^k})') \left(\frac{\sum\limits_{n\in\mathcal{T}^k}(d_n)}{\sum\limits_{n=1}^{N}(d_n)}\right), \tag{9}$$

[Step 3] Assign $\{\boldsymbol{x}_1, \boldsymbol{x}_2...\boldsymbol{x}_N\}$ users to K clusters $\{\mathcal{T}^1, \mathcal{T}^2...\mathcal{T}^K\}$ based on the minimum distance between the users and cluster centre using $\mathfrak{R}_{K\times N}$.

[Step 4] Compute new cluster centres $\{\boldsymbol{c}_{\mathcal{T}^1}, \boldsymbol{c}_{\mathcal{T}^2}...\boldsymbol{c}_{\mathcal{T}^k}\}$ by using,

$$\boldsymbol{c}_{\mathcal{T}^k} = \frac{1}{\sum\limits_{n\in\mathcal{T}^k} d_n}\sum_{n\in\mathcal{T}^k} d_n\mathbf{x}_n. \tag{10}$$

end while

To have a fair comparison between the conventional 6 beams of fixed beam design, we use Voronoi Tessellation [17] and generate convex polygons around the previously obtained clusters, such that, all the area covered by the benchmark design is covered by the proposed adaptive scheme. Any centre $\boldsymbol{c}_{\mathcal{T}^k}$ is simply a point in the Euclidean plane, and its corresponding Voronoi cell V_u consists of every point in the Euclidean plane whose Euclidean distance to $\boldsymbol{c}_{\mathcal{T}^u}$ is less than or equal to its Euclidean distance to any other centre $\boldsymbol{c}_{\mathcal{T}^{v\neq u}}$.

The Voronoi cells are convex polygons because each cell is obtained from the intersection of geometric half-spaces. The collection of such convex Voronoi polygons of the 6 reference beams is shown by red convex polygons in Figure 3. We approximate the boundary of Voronoi polygons as beam contour and the geographic centres $\{\boldsymbol{c}'_1, \boldsymbol{c}'_2...\boldsymbol{c}'_K\}$ of Voronoi polygons as beam centres.

Furthermore, from the perspective of antenna pattern design, the irregular Voronoi polygons cannot be approximated as beam footprints. Also, considering the mathematical tractability and topological packing, we approximate the convex polygons into ellipses as shown in [18]. The centres of the thus obtained ellipses $(\boldsymbol{c}_1, \boldsymbol{c}_2...\boldsymbol{c}_k)$ will represent the proposed adaptive beams centres. The semi-major and semi-minor axis of the approximated ellipses defines the boundary of the proposed adaptive beams. The angle of rotation of approximated ellipses represents the orientation of the proposed adaptive beams. The approximated beams are denoted using green ellipses in Figure 3.

Finally, for comparison with the benchmark, the elliptical beam pattern is obtained by approximating the antenna gains using two-dimensional Gaussian elliptical function. The antenna gain at any point of the elliptical beam could be modelled using,

$$f(x,y) = A\exp(-(m_1(x-x_o)^2 + 2m_2(x-x_o)(y-y_o) + m_3(y-y_o)^2)), \tag{11}$$

where the matrix $\begin{bmatrix} m_1 & m_2 \\ m_2 & m_3 \end{bmatrix}$ is positive-definite matrix [19].

The semi-major and semi-minor axis of the ellipses are fitted with σ_X and σ_Y of elliptical Gaussian function. The Gaussian function is phase rotated with angle φ to fit the orientation of the ellipse. The coefficient A is the maximum antenna gain or the amplitude of boresight point which is chosen inline with the boresight antenna gain of the benchmark. The centre of the Gaussian function (intersection point of σ_x and σ_y) is the centre $(c_k = x_0, y_0)$ of the ellipse. The values of $m1, m2$ and $m3$ are defined using,

$$m_1 = \frac{\cos^2\varphi}{2\sigma_X^2} + \frac{\sin^2\varphi}{2\sigma_Y^2}, \tag{12a}$$

$$m_2 = -\frac{\sin 2\varphi}{4\sigma_X^2} + \frac{\sin 2\varphi}{4\sigma_Y^2}, \tag{12b}$$

$$m_3 = \frac{\sin^2\varphi}{2\sigma_X^2} + \frac{\cos^2\varphi}{2\sigma_Y^2}. \tag{12c}$$

B. Demand-Aware User Scheduling

Conventional scheduling techniques such as [12], [20] focus on selecting users with orthogonal channel vectors at any time t. Even though such approach will help precoding to successfully mitigate interference, it might fail to satisfy the

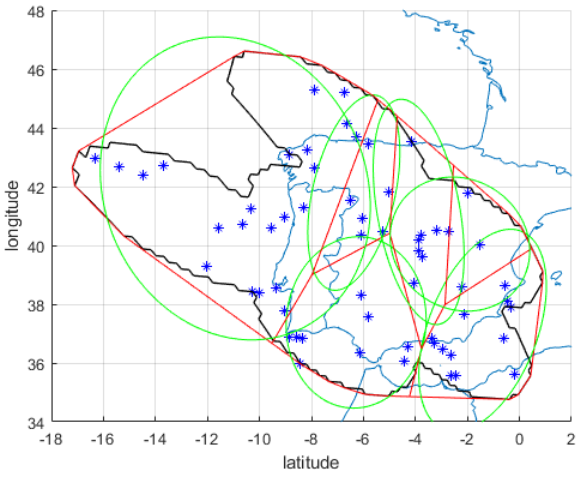

Fig. 3. Demand-Aware Adaptive Beam Footprint

individual user demand request. To overcome this, we use a demand-Aware user scheduling, which essentially targets the selection of a set $\mathcal{U} = \{U_1, U_2...U_k\}$, containing *K* users from the pool of *M* users at each scheduling time, $t = 1, ..., T$ for all the *K* beams such that d_m, $\forall m$, is met at the end of T time period. Furthermore, to make sure that precoding still provide meaningful gains, the proposed demand-Aware scheduling also considers the channel orthogonality.

However, obtaining the optimal scheduling solution is a combinational problem and requires an exhaustive search-based user grouping and scheduling, which quickly become impractical due to exponential complexity. Hence, we use weighted semi-orthogonal scheduling [11] which is a sub-optimal heuristic method that uses both user demand and channel orthogonality. The Demand-Aware User Scheduling as shown in Algorithm 2, produces a schedule user set ($\mathcal{U} = \{U_1, U_2...U_k\}$) such that the channel vectors of the users in $\mathcal{U}$ are as orthogonal as possible using cosine similarity as,

$$\frac{|\,\mathbf{h}_1^H \mathbf{h}_2\,|}{\|\mathbf{h}_1\|\|\mathbf{h}_2\|} = \begin{cases} 1 & \text{Similar channel vectors} \\ 0 & \text{Orthogonal channel vectors} \end{cases} \tag{13}$$

and also ensures that the demand d_m of every user m is lesser or equal to the offered throughput using demand priority coefficient α_m. Furthermore, we consider unicast scheduling and hence one user per beam is selected.

IV. Numerical Evaluation

In this section, we evaluate the proposed demand-Aware approaches with respect to conventional fixed approaches. Accordingly, the results are evaluated using four cases mentioned in Table I.

In the first case, we consider 6 beams of conventional fixed beam design provided by European Space Agency (ESA) [13], [21] and a well known semi-orthogonal scheduling as a benchmark [12]. In case 2, we introduce demand driven adaptability at only user scheduling level. In case 3, we use demand driven adaptability only for beam designing. In case 4, we use demand-Aware adaptability at both beam design and user scheduling.

Algorithm 2 Demand-Aware User Scheduling

[Step 1] Compute the initial demand priority coefficient at $t = 1$ for every user m using,
$\alpha_m(t=1) = \frac{d_m(t=1)}{max_m(d_m(t=1))} \leftarrow \forall m$ where $\alpha_m \in [0, 1]$
[Step 2] Initialize the set of indexes of the previously scheduled users using, $\Lambda = \emptyset$
[Step 3] Perform user scheduling. For every value of t, select K users.
for $t = 1$ to T **do**
  [Step 3.A] Select first user using,
  for $m = 1$ to M **do**
    $U_1 = \max(\alpha_m(t).\|\mathbf{h}_m\|)$
  end for
  Update Λ to avoid reselection of already scheduled user using, $\Lambda = \Lambda \in U_1$
  [Step 3.B] Select the remaining $(K-1)$ users using,
  for k = 2 to K **do**
    for m = 1 to M **do**
    w_m = $\max(\alpha_m(t).(1 - \sum_{j\in\Lambda} \frac{|\mathbf{h}_j \mathbf{h}_m^H|}{\|\mathbf{h}_j\|\|\mathbf{h}_m\|}))$
    end for
    U_k is the user *m* of w_m.
    Update set: $\Lambda = \Lambda \in U_k$
  end for
  [Step 4] Update demand priority coefficient based on the average offered rate using α_m such that $\alpha_m(t) = \frac{d_m(t)}{E_m[R_m(t)]}$
end for=0

TABLE I
Cases Evaluated

	Case 1	Case 2	Case 3	Case 4
Conventional Fixed Beam Design	✓	✓		
Demand-Aware Beam Design			✓	✓
conventional Fixed Scheduling	✓		✓	
Demand-Aware Scheduling		✓		✓

A. Simulation Parameters

The simulation parameters and the link budget are as shown in Table II we consider a total number of $M = 60$ users distributed across $K = 6$ beams. Users locations and demands have been extracted from the SnT traffic simulator [22]. Furthermore, we consider a sum power-constrained system with a per-beam power of 20 dBW and a bandwidth of 500 MHz.

B. Beam level Demand Satisfaction

Demand satisfaction at beam level can be defined as the difference between the average beam demand and average beam

TABLE II
SIMULATION PARAMETERS

Satellite longitude	13 degree East (GEO)
Satellite total radiated power, P_T	6000 W
Total Number of Beams, N_B	71 (Only 6 beams are considered)
Number of HPA, N_{HPA}	36 (2 beams per HPA)
Beam Radiation Pattern	Provided by ESA
Downlink carrier Frequency	19.5 GHz
User link bandwidth, B_W	500 MHz
Roll-off Factor	20%
Duration of time slot. T_{slot}	1.3 ms
Number of time slots	100
Antenna Diameter	0.6
Terminal antenna efficiency	60%
DL wavelength	0.01538 m

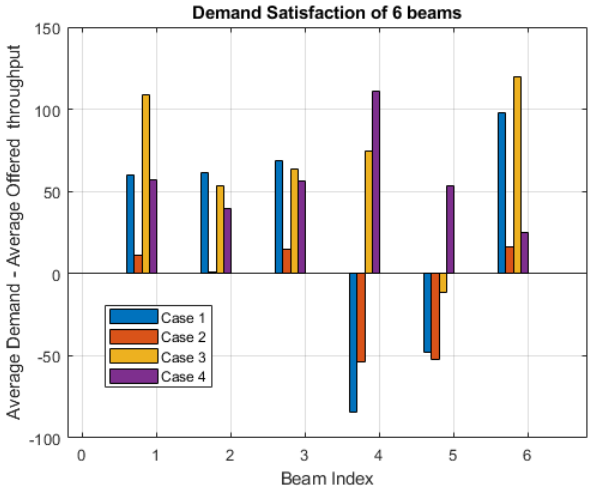

Fig. 4. Beam-level Demand Satisfaction

offered throughput. Accordingly, Figure 4 provides demand satisfaction of 6 beams for the previously defined four cases. In case 1, where demand is not considered during beam design and user scheduling, demand satisfaction is not achieved for beam 4 and beam 5. In case 2, when demand awareness is considered for only user scheduling, beam demand is again not met for beams 4 and 5. This is because, due to uneven demand distribution among the 6 beams, the beam 4 and 5 have high demand to be met and demand-Aware user scheduling fails to meet demand of such beams. This can be verified in Figure 5 which shows the distribution of total system demand across the 6 beams. The conventional fixed beam design will result in some beams overload with high demand to meet and leave some beams underused. Also, the demand-Aware beam design will distribute the beam demand more equally among all the beams. Hence all the beams will have similar demand to be met. This can be verified by the Case 3 plots in Figure 4. The demand satisfaction is considerably improved as only beam 5 not been satisfied with a very small margin. However, in case 4, when we use demand awareness in both beam design and user scheduling, the demand of all the beams are satisfied.

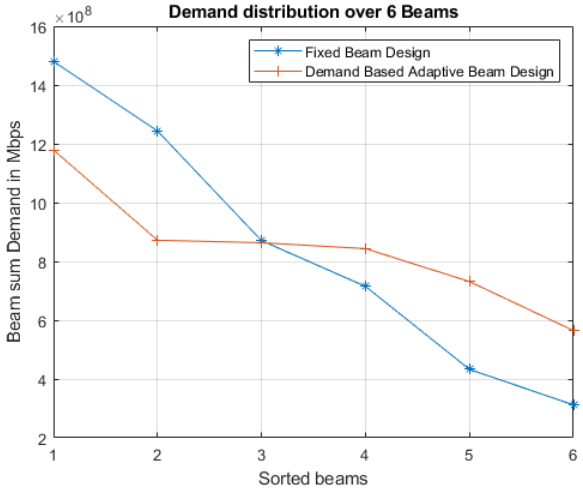

Fig. 5. Demand Distribution across all 6 beams

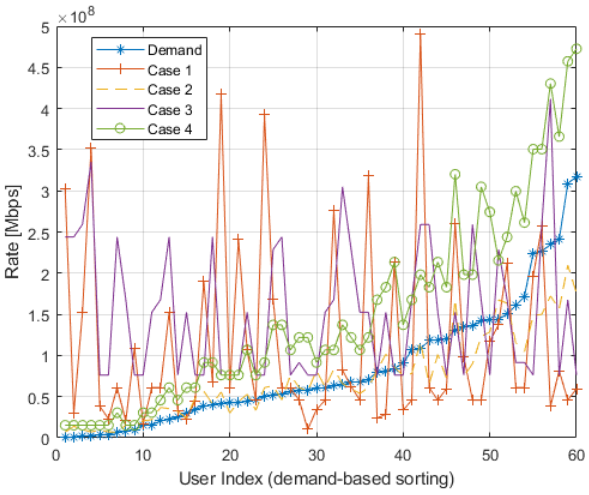

Fig. 6. User-level Demand Satisfaction

C. User level Demand Satisfaction

Demand satisfaction at user level can be defined as the difference between the average user demand and average user offered throughput. Accordingly, Figure 6 provides demand satisfaction of 60 users. Clearly, the conventional Case 1 that does not consider demand for either beam design and user scheduling performs worst. In Case 2, when demand is considered only at user scheduling, the average offered throughput follows the demand curve. However, Many users with high demand are not satisfied. In Case 3, where demand is considered only for beam footprint planning, the user level demand satisfaction is poor but better than the Case 1. Finally, the Case 4 which uses demand at both beam design and scheduling performs best by both following the demand curve and satisfying the user demand at all cases.

V. Conclusion

Contrary to the current state-of-the-art solutions, we consider the actual user demand requirements in both beam planning and user scheduling. In this work, we show the benefits in terms of user demand satisfaction and beam demand satisfaction of the proposed beam design and user scheduling. In particular, the conventional systems face unbalanced situations with significant amounts of unmet capacity, while in our case, the users' demand requests and beams' demand requests have been met.

References

[1] S. K. Rao, "Advanced antenna technologies for satellite communications payloads," *IEEE Transactions on Antennas and Propagation*, vol. 63, no. 4, pp. 1205–1217, 2015.

[2] H. Al-Hraishawi, E. Lagunas, and S. Chatzinotas, "Traffic simulator for multibeam satellite communication systems," in *2020 10th Advanced Satellite Multimedia Systems Conference and the 16th Signal Processing for Space Communications Workshop (ASMS/SPSC)*, 2020, pp. 1–8.

[3] P. J. Honnaiah, N. Maturo, S. Chatzinotas, S. Kisseleff, and J. Krause, "Demand-based adaptive multi-beam pattern and footprint planning for high throughput geo satellite systems," *IEEE Open Journal of the Communications Society*, vol. 2, pp. 1526–1540, 2021.

[4] G. Maral, M. Bousquet, and Z. Sun, *Satellite communications systems: systems, techniques and technology*. John Wiley & Sons, 2020.

[5] D. Digdarsini, M. Kumar, and T. Ram, "Design amp; hardware realization of fpga based digital beam forming system," in *2016 3rd International Conference on Signal Processing and Integrated Networks (SPIN)*, 2016, pp. 275–278.

[6] J. Krivochiza, J. C. M. Duncan, J. Querol, N. Maturo, L. M. Marrero, S. Andrenacci, J. Krause, and S. Chatzinotas, "End-to-end precoding validation over a live geo satellite forward link," *IEEE Access*, pp. 1–1, 2021.

[7] M. Vázquez, A. Pérez-Neira, D. Christopoulos, S. Chatzinotas, B. Ottersten, P.-D. Arapoglou, A. Ginesi, and G. Taricco, "Precoding in multibeam satellite communications: Present and future challenges," *IEEE Wireless Communications*, vol. 23, no. 6, pp. 88–95, 2016.

[8] C. SWANNACK, "Low complexity multiuser scheduling for maximizing throughput in the mimo broadcast channel," in *Proc. Allerton Conf. Commun., Control, Comput., Allerton, IL, Oct. 2004*, 2004, pp. 440–449.

[9] G. Taricco and A. Ginesi, "Precoding for flexible high throughput satellites: Hot-spot scenario," *IEEE Transactions on Broadcasting*, vol. 65, no. 1, pp. 65–72, 2019.

[10] A. Bandi, M. R. B. Shankar, S. Chatzinotas, and B. Ottersten, "Joint user grouping, scheduling, and precoding for multicast energy efficiency in multigroup multicast systems," *IEEE Transactions on Wireless Communications*, vol. 19, no. 12, pp. 8195–8210, 2020.

[11] P. J. Honnaiah, E. Lagunas, D. Spano, N. Maturo, and S. Chatzinotas, "Demand-based scheduling for precoded multibeam high-throughput satellite systems," in *2021 IEEE Wireless Communications and Networking Conference (WCNC)*, 2021, pp. 1–6.

[12] T. Yoo and A. Goldsmith, "On the optimality of multiantenna broadcast scheduling using zero-forcing beamforming," *IEEE Journal on Selected Areas in Communications*, vol. 24, no. 3, pp. 528–541, 2006.

[13] D. Christopoulos, S. Chatzinotas, and B. Ottersten, "Multicast multigroup precoding and user scheduling for frame-based satellite communications," *IEEE Transactions on Wireless Communications*, vol. 14, no. 9, pp. 4695–4707, 2015.

[14] C. Peel, B. Hochwald, and A. Swindlehurst, "A vector-perturbation technique for near-capacity multiantenna multiuser communication-part i: channel inversion and regularization," *IEEE Transactions on Communications*, vol. 53, no. 1, pp. 195–202, 2005.

[15] S. Lloyd, "Least squares quantization in pcm," *IEEE Transactions on Information Theory*, vol. 28, no. 2, pp. 129–137, 1982.

[16] D. Arthur and S. Vassilvitskii, "K-means++: the advantages of careful seeding," in *In Proceedings of the 18th Annual ACM-SIAM Symposium on Discrete Algorithms*, 2007.

[17] M. L. Gavrilova, Ed., *Generalized Voronoi Diagram: A Geometry-Based Approach to Computational Intelligence*. Springer Berlin Heidelberg, 2009. [Online]. Available: https://doi.org/10.1007/978-3-540-85126-4

[18] E. W. Weisstein. Polygon to ellipse approximation, MathWorld: A Wolfram Web Resource. [Online]. Available: https://mathworld.wolfram.com/Ellipse.html

[19] N. Nawri. Berechnung von Kovarianzellipsen, Web Resource. [Online]. Available: http://imkbemu.physik.uni-karlsruhe.de/ẽisatlas/covariance_ellipses.pdf

[20] G. Taricco, "Linear precoding methods for multi-beam broadband satellite systems," in *European Wireless 2014; 20th European Wireless Conference*, 2014, pp. 1–6.

[21] "Flexpredem - demonstrator of precoding techniques for flexible broadband systems," *Activity Code: 3C.014*. [Online]. Available: https://artes.esa.int/projects/flexpredem

[22] H. Al-Hraishawi, E. Lagunas, and S. Chatzinotas, "Traffic simulator for multibeam satellite communication systems," 2020.